Disorder-induced crossover of Mott insulator to weak Anderson localized regime in an argon-irradiated $NdNiO_3$ film

Ravindra Singh Bisht,[1,*] Sudipta Chatterjee,[1] Sreyan Raha,[2] Achintya Singha,[2] D. Kabiraj,[3] D. Kanjilal,[3] and A. K. Raychaudhuri[4,†]

[1]*Department of Condensed Matter Physics and Materials Science, S.N. Bose National Centre for Basic Sciences, JD Block, Sector III Salt Lake, Kolkata 700106, India*

[2]*Department of Physics, Bose Institute, 93/1, Acharya Prafulla Chandra Road, Kolkata 700009, India*

[3]*Materials Science Division, Inter University Accelerator Centre, Aruna Asaf Ali Marg, New Delhi 110067, India*

[4]*CSIR-Central Glass and Ceramic Research Institute, 196 Raja S.C. Mullick Road, Kolkata 700032, India*

(Received 3 January 2022; revised 7 April 2022; accepted 6 May 2022; published 16 May 2022)

We show that an introduction of disorder in a controlled way using 1 MeV argon (Ar) ion irradiation, suppresses the correlation driven metal-insulator transition (MIT) in $NdNiO_3$ films. The films make a crossover to a heavily disordered conductor governed by weak localization (WL) and at even higher disorder, an Anderson localized state. The disorder (atomic displacement up to 2% of the total atoms) in the $NdNiO_3$ films was created using 1 MeV Ar^{4+} ion irradiation. We show that the pristine films of $NdNiO_3$ exhibit an MIT with the conduction process being governed by variable range hopping (VRH). For disorder up to 1% of the displaced atoms or lower, the insulating state arising from a gap in the density of states (DOS) at the Fermi level (E_F) as in a Mott insulator is suppressed and the conduction in the film shows a WL behavior with finite conductivity at temperature $T \to 0$. This behavior is expected in a disordered conductor that does not have a gap in DOS at E_F. At higher fluences the conductivity reduces substantially but the electrical conduction shows a power-law temperature dependence with a small but finite zero temperature conductivity $\sigma(T = 0)$ which is expected in a solid with electrons that are Anderson localized. A similar experiment was performed on the La substituted $NdNiO_3$ films ($Nd_{1-x}La_xNiO_3$) with $x = 0.3$ that are grown in the same way. La substitution in $NdNiO_3$ suppresses the temperature driven transition and leads to a metallic state with critical composition at $x \approx 0.3$. The pristine as well as films irradiated with lowest fluence shows metallic or marginally metallic behavior grown on $LaAlO_3$ and $SrTiO_3$ substrates, respectively. However, at higher fluences they too exhibit a convergence in electronic transport and σ shows a power-law temperature dependence at low T with $\sigma(T = 0) \neq 0$. Evidence of suppression of correlated behavior can also be seen in the irradiated films where the non-Gaussian nature of resistance fluctuation at $T \approx T_{MI}$, a signature of correlated electron systems, is suppressed on irradiation that leads to collapse of the MIT. Evidence for progressing disordering of the films on irradiation were observed in Raman spectroscopy as well as x-ray studies that show the basic integrity of the NiO_6 octahedra is preserved and the structure retains its crystallinity.

DOI: 10.1103/PhysRevB.105.205120

I. INTRODUCTION

Metal-insulator transition (MIT) is a fascinating phenomenon where a metal with electrons that have extended wave functions enter into an insulating state that have strongly localized electrons when one or more physical parameters are varied [1–5]. In one class of MIT, the transition is principally governed by a crystallographic transition that leads to opening of a gap in the conduction band leading to a change in the density of states (DOS) at the Fermi level (E_F) as a result of the change in lattice symmetry [6]. In another class of MIT, which has been widely researched currently, is an electronic transition. This type of MIT is generally classified in two broad classes. One class is the correlation driven transition (like a Mott type transition) where the DOS develops a gap so that the DOS at E_F, $g(E_F) = 0$. The transition is first order in nature and the MIT is observed as a function of temperature [1,7,8].

The other broad class is the disorder driven Anderson transition where the electronic states around the E_F are localized although $g(E_F)$ remains finite, i.e., $g(E_F) \neq 0$ [9,10]. The MIT can be ushered in through tuning the disorder parameter Δ. The transition to the insulating state occurs when the disorder parameter scaled by the bandwidth B, $\delta \equiv \frac{\Delta}{B}$, reaches a critical value $\delta_c \sim 1$. Similarly, for the correlation driven transitions, the scaled parameter $u \equiv \frac{U}{B}$ is tuned which measures the on-site Coulomb repulsion U and the transition occurs at a critical value $u_c \sim 1$ [1,7,8]. Extensive investigations that have been undertaken over the years have established that in a real physical system the transition has aspects of both disorder and correlation. Finite values of both δ and u make the phenomena complex, in particular when both disorder and correlation have comparable strengths ($\delta \sim u$) and the parameters are close to their critical values [11]. The MIT

*ravindrasinghbisht91@gmail.com
†arupraychaudhuri4217@gmail.com

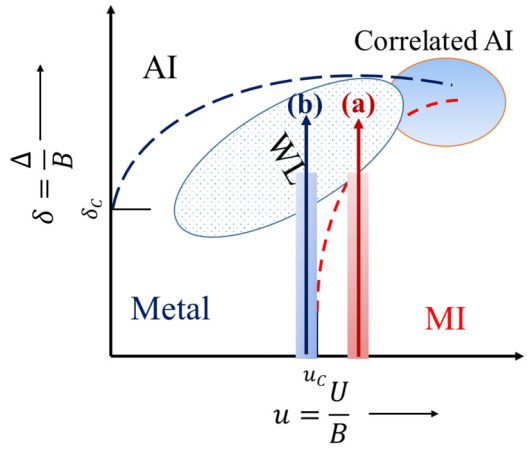

FIG. 1. Schematic of the phase diagram with correlation and disorder: MI: Mott insulator, AI: Anderson insulator, WL: weak localization regime. The vertical arrows show the schematic path of disordering by 1 MeV Ar ions for (a) $NdNiO_3$ (NNO) film and (b) $Nd_{0.7}La_{0.3}NiO_3$ film. Shading around the arrows show expected variations arising from the strain for films grown on different substrates. The phase diagram has been adapted from [13].

in case of a Mott transition with disorder is referred to as Anderson-Mott transition. Though the problem is complex, there are certain unifying scenarios that have emerged over the years. For instance, it has been shown that destabilization of the gapped insulating state beyond a certain level of disorder can lead to a crossover of insulating to a correlated disordered metallic state which at an even higher level of disorder δ can change over to an Anderson insulator (AI) [12–14]. At zero temperature [12], as well as at finite but low temperature [13], phase diagram with parameters δ and u have been proposed [15], which shows how a gradual enhancement of δ can drive a Mott insulator (with $u > u_C$) to a disordered metallic state and eventually to AI depending on the values of the parameters δ and u. For ease of discussion, a schematic phase diagram adapted from Ref. [13] is shown in Fig. 1. It is noted that although the phase diagram has been developed in the context of the Mott-Anderson MIT, it can also be adopted to describe how the level of the disorder can change a correlation-driven MIT. The specific context of the Mott insulator is used to represent a general class of such transitions.

We place the schematic of a qualitative phase diagram in Fig. 1 in perspective of the experimental realization proposed in this paper. If we start from a region deep inside the insulating region where $u > u_c$ and enhance the disorder thus tuning δ, it would be possible to crossover to a region of AI or at least a region of weakly localized metal for sufficiently large δ. The disordering path following vertical (a) can be realized if the process of disordering does not affect u. In this case it is expected that when the crossover occurs, the conductivity would increase on collapse of the gapped insulator as the gap at E_F closes and with further increase in the disorder, the conductivity would go down again.

It will be also interesting to explore when such a process of disordering is following vertical (b), where the starting sample is not in a gapped insulating state but in a weakly localized regime lying close to the critical boundary ($u \geqslant u_c$). In this case the disordering following vertical (b) would lead to a continuous decrease of conductivity due to enhancement of disorder as there is no crossover involved unlike the disordering following vertical (a). Thus there will be qualitative differences expected to be observed when the disordering occurs following vertical (a) and (b).

One way to introduce disorder in a system is through substitution of isovalent ions with different ionic radii [2,16,17]. This method though widely used has co-lateral problems of change in the crystal structure and the changes in ionic radii can create internal pressure leading to change in bandwidth B. This would not only change δ but also can change u as well. A cleaner method to vary δ only and move along vertical (a) and (b) in Fig. 1 is to use energetic heavy ion irradiation in a controlled way as a tool to create disorder without changing the chemistry. Ion irradiation at high energy has the ability to create high density defects in a short time. When the sample used is thin enough (like a thin film on a substrate) the projected ions do not stop inside the film and, as a result, the irradiation does not change the chemistry. Thus an extremely useful investigation will be to use irradiation to create controlled disorder and investigate the progressive destabilization of the gapped insulator as proposed in the schematic shown in Fig. 1. In particular, it will be important to explore the nature of the electrical conduction in the solid when the insulating state is suppressed by disorder.

Investigation of disordering a Mott insulator using x-ray irradiation has been done in strongly correlated organic conductors [18]. The radiation induced disorder enhances the conductivity but the insulating state is retained at low temperature. The disordered insulating state can be made to change over to a weakly localized conducting state at low temperature using hydrostatic pressure that enhances the conduction bandwidth by enhancing the transfer integral. Though high energy, swift heavy ions have been used in the past to disorder oxides like $NdNiO_3$ film, these investigations did not address the issue of collapse of an insulating state like a Mott insulator when it is disordered progressively [19–21]. The energy of the ions used in these investigations were very high (200 MeV). In these energy ranges the defects created are of different nature due to predominance of the electronic energy loss mechanism.

In the present work we have investigated the disordering of $NdNiO_3$ (NNO) films of thickness ≈15 nm which were grown on (001) oriented crystalline substrates $LaAlO_3$ (LAO) and $SrTiO_3$ (STO) using 1 MeV Ar ions. The stopping distance of 1 MeV Ar ions in such oxides is ≈500 nm, which is much greater than the film thickness. Thus the ions do not stop inside the film, instead they stop deep in the substrate. The path of disordering thus follows the vertical (a) marked in Fig. 1.

The $RNiO_3$ (R = rare earth except for La) are known to exhibit a first order MIT. The MIT is also accompanied by a structural change from high temperature orthorhombic phase to a low temperature monoclinic phase [22,23]. Different scenarios have been addressed in the literature to understand the nature of the insulating state in $RNiO_3$. However, the exact mechanism is still elusive and debatable [22–24]. One scenario proposed that a charge disproportionate Ni site can be responsible for the charge ordering in nickelates [25]. Charge ordering in $RNiO_3$ has also been proposed as a cause

TABLE I. Details of the samples (and acronyms), the fluence used in the experiment, and the disorder (atomic displacement) generated are summarized.

Fluence (cm^{-2})	Disorder (%)	Film NNO/STO	Film NNO/LAO	Film NLNO/STO	Film NLNO/LAO
0	0	NNO/S0	NNO/L0	NLNO/S0	NLNO/L0
1×10^{14}	0.2	NNO/S1	NNO/L1	NLNO/S1	NLNO/L1
5×10^{14}	1.0	NNO/S2	NNO/L2	NLNO/S2	NLNO/L2
1×10^{15}	2.0	NNO/S3	NNO/L3	NLNO/S3	NLNO/L3

of the MIT which is a result of a site selective Mott phase [24]. Experimental evidence has been advanced for a negative charge transfer scenario for the MIT the $RNiO_3$ [26]. In the present study we put the $RNiO_3$ close to the Mott insulators, although we are aware that $RNiO_3$ may not be the best example for a Mott system.

We have also done similar ion irradiation induced disordering on a film of $Nd_{0.7}La_{0.3}NiO_3$ (NLNO), which is close to the critical region of MIT achieved by substitution of Nd with La [27,28]. ($Nd_{1-x}La_xNiO_3$) film shows substitution induced MIT due to bandwidth change close to a critical concentration $x \equiv 0.3$–0.35, whose exact value depends on the strain arising from the substrate. The first order MIT in $NdNiO_3$ changes its nature when Nd is substituted by La close to the critical region of a composition driven MIT as in an Anderson type transition [28]. Thus the disordering of NLNO films by Ar irradiation follows path (b) in Fig. 1. Suppression of Mott transition where a substitution induced closing of gap at E_F has also been reported in $Sr_3(Ir_{1-x}Ru_x)_2O_7$, the introduction of disorder can lead to opening up of a gap with power-law nature in the system on Ru substitution [29]. The observations made by us in this investigation by ion irradiation has similarity with the observation above.

The experimental results obtained in this investigation establish broad validity of the qualitative phase diagram as shown in the schematic in Fig. 1 which has been adapted from earlier theoretical investigations on Mott-Anderson transitions [13]. The present investigation showed that ion induced disordering even at low fluence does suppress the insulating phase leading to a weakly localized regime at low irradiation fluence where the resistivity (ρ) shows a negative temperature coefficient (NTC) ($\frac{d\rho}{dt} < 0$) but a finite zero temperature conductivity [$\sigma(T = 0) \neq 0$]. In fact, for the films disordered at low fluence, the resistivities at low temperature are even less than that of the pristine film which show a MIT.

II. EXPERIMENT

The NNO and NLNO films of thickness ≈15 nm were prepared by a 248 nm KrF pulsed laser deposition (PLD) and the growth of the films were monitored by *in situ* reflection high energy electron diffraction (RHEED) which also was used to determine the thickness of the films from the number of oscillations in RHEED intensity. The films were grown at a temperature of 625 °C and a oxygen pressure of 0.11 Torr. The laser fluence during deposition was nearly 2.5 J/cm^2. More details on the characterizations have been given in Refs. [30,31].

The ion irradiation was performed in the electron cyclotron resonance (ECR) ion source based irradiation facility using 1 MeV Ar^{4+} ions with a beam current of 250 particle nA (pnA). The details are given in Sec. S1 of the Supplemental Material [32]. The range of 1 MeV Ar ions in materials like NNO, STO, and LAO is ≈490–500 nm. Since this is greater than the film thickness, the ions stop deep in the substrate after disordering the film. The film gets progressively disordered by the irradiation but it has no implanted Ar. For the energy of the Ar ions used, the energy loss is primarily nuclear in nature creating direct displacement of ions from the lattice sites. The number of vacancies created by the Ar ions in NNO were calculated by using TRIM [33]. The total knocked out atoms (atomic displacements) is ≈3.5×10^{22}/cm^3 for a fluence of 1×10^{15}/cm^2. In general ≈99% of the damage anneals instantly at room temperature and the nominal vacancy created for the fluence is 0.35 vacancies/target atom [33]. The retention after thermal annealing ≈3.5×10^{20}/cm^3. Scaling by the atomic density leads to a disorder in the NNO film of nearly 2%. In Table I we summarize the details of the samples (and acronyms), fluences used in the experiment, and the disorder (atomic displacement) generated.

After the irradiation, samples were characterized by x-ray diffraction (XRD) and Raman spectroscopy along with the pristine films to ascertain progressive disordering as the fluence is increased. Raman data were taken using LABRAM HR micro-Raman setup with an Ar ion laser (wavelength 488 nm) as an excitation source. Resistivity (ρ) measurements were performed in a collinear four-probe geometry down to nearly 3 K in a pulsed tube cryocooler. The Cr/Au contact pads deposited through a shadow mask on the films using a thermal evaporator were used for making electrical contacts. The $\frac{1}{f}$ noise measurement was taken in a four-probe geometry using an AC biased, digital signal processing technique [34–36]. The details of measurement technique and data analysis are given in Sec. S2 of the Supplemental Material [32].

III. RESULTS

A. Structural data

The θ-2θ XRD scans taken on the pristine and irradiated films show that films are free from any impurity phase and the texture of the film is maintained. Due to the lattice mismatch of films (NNO and NLNO) with LAO [a_{pc} (Å) ≈3.79] and STO [a_{pc} (Å) ≈3.90], the films grown on them will experience an in-plane compressive and tensile strain, respectively (a_{pc} denotes a pseudocubic lattice constant). In Figs. 2 and 3 we show the XRD scans of the pristine and irradiated films around

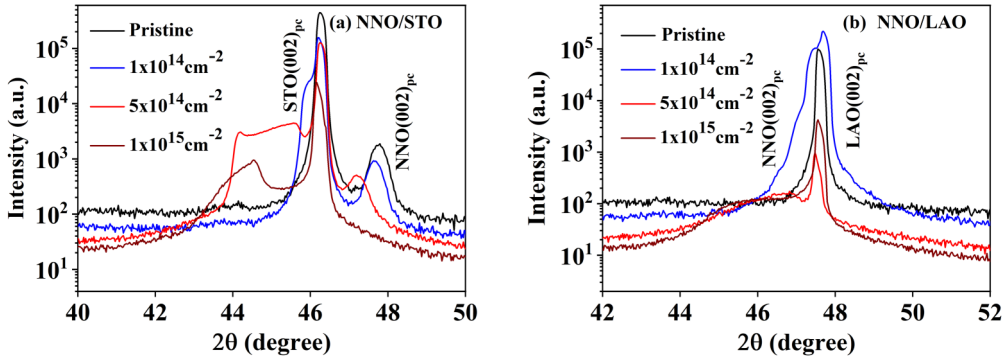

FIG. 2. X-ray diffraction around indices (002) in pristine and irradiated films of NNO grown on (a) STO and (b) LAO. (Full range data are in Fig. S3 [32]).

the most prominent (002) peaks. The full range scans are shown in the Supplemental Material as Figs. S3 and S4 [32]. An additional feature in the substrate peaks has been observed for all the samples except the pristine films. The extra feature in the Bragg peak of the substrate can be attributed to the x-ray scattering from the damaged region of the underlying substrate upon ion irradiation. The stopping of the ions within the substrates leads to strain within it. As an example, this has been observed for the titanium irradiated $SrTiO_3$substrate [37]. The growth directions of the films have been marked as $(002)_{pc}$, where subscript pc represents pseudocubic notation. The line positions ($2\theta_{002}$) and the FWHM values ($\Delta 2\theta_{002}$) of the XRD lines corresponding to the (002) indexed lines of the films are summarized in Table S1 [32]. The positions of the (002) peaks show that in NNO/S0 the out-of-plane (in-plane) lattice constant is smaller (larger) than NNO/L0. Thus there is a small in-plane compressive strain in the NNO/L0 film. The shifts of the XRD peaks to the lower 2θ values on progressive irradiation show that the out-of plane (in-plane) lattice parameters experiences an expansion (compression). The line shifts on irradiation, however, are small and the shifts are within 1% to 2%. For highest values of fluence the designated (002) lines in both NNO and NLNO films grown on STO show distortions. It may be suggested that the contraction in the lattice occurs due to creation of vacancy by the irradiation and the resulting relaxation of the lattice around the vacancy. This is expected also to enhance the FWHM of the XRD peaks as observed. Retention of the Bragg peaks upon irradiation show that the films retain their crystallinity albeit with disorder.

The structural evolution and the integrity of the NNO structure in the irradiated films were investigated by Raman spectroscopy, which is a local structure sensitive tool and can give information to what happens to the NiO_6 octahedron that is at the core of the NNO structure. The strong Raman signal from the LAO substrate ensures that the Raman spectra are collected from scattered light that covers the complete thickness of the film and a part of the substrate. At room temperature the crystal structure of NNO is orthorhombic (*Pbnm*). From group theoretical considerations, there are 24 Raman active modes that have been predicted for the structurally distorted oxides like NNO [38]. However, experimentally only a few Raman modes have been observed and our data are consistent with the earlier reports [39,40]. The major observed modes have E_g and A_g symmetries which are related to the NiO_6 octahedra. Any changes in these modes as revealed through the Raman spectroscopy data would give information in the structural integrity of the NiO_6.

In Figs. 4(a) and 4(b) we show the Raman spectra for the pristine and irradiated films of NNO and NLNO grown on LAO. (Note: Due to the high background from STO substrate and small thickness of the film the Raman modes of NNO and NLNO films grown on STO substrates were too weak to detect.) The positions of the Raman lines as measured in pristine and irradiated films along with the modes assigned

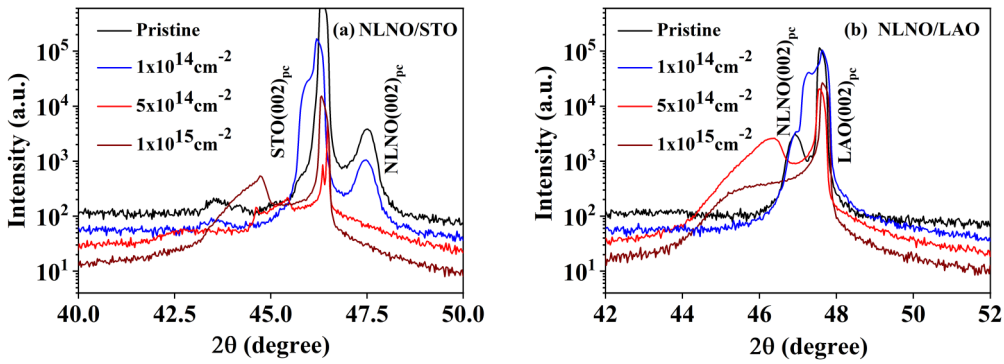

FIG. 3. X-ray diffraction around indices (002) in pristine and irradiated films of NLNO grown on (a) STO and (b) LAO. (Full range data are in Fig. S4 [32]).

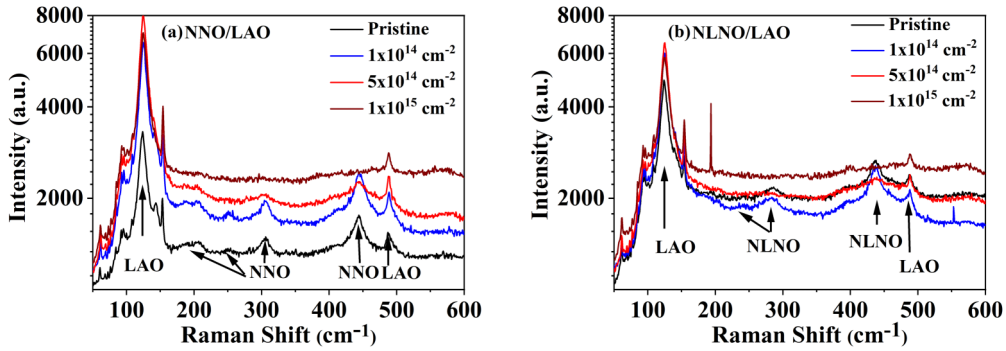

FIG. 4. Raman spectra on pristine and irradiated films on LAO substrate for (a) NNO and (b) NLNO. Progressive smearing of the NNO peaks on disordering can be seen.

are summarized in Table S1 [32]. The positions of the Raman modes in NNO/L0 and NLNO/L0 are comparable to the reported values in films [40] and bulk [38]. In NNO/L0 the most intense peak at 443.9 cm^{-1} and the weak shoulder at 431 cm^{-1} arise from E_g modes, where the former is bending of the NiO_6 octahedral cage and the later is a breathing mode with out-of-phase oscillation of apical and basal plane oxygens. The medium strong line at 305.5 cm^{-1} with a weak companion line at 251 cm^{-1} in NNO/L0 arise from A_g modes that represent octahedral rotation out-of-phase and in-phase, respectively. The weaker peaks at smaller wavelengths arise from these modes as well. The corresponding Raman modes in NNO/L0 soften in NLNO/L0 on addition of La that makes the Ni-O bond length larger. In addition some of the weak lines in NNO/L0 could not be detected in NLNO/L0 [40].

On irradiation most of the Raman lines soften by a small amount. For some of the Raman lines there are negligible changes (<0.5%) for fluences $\leqslant 5 \times 10^{14}$ cm^{-2} although the intensity of the lines decrease along with line broadening as measured by the full-width at half-maxima (Table S2) [32]. The observation of retention of the Raman lines (albeit widened) at relatively lower fluences shows that the integrity of the metal-oxide octahedra is mostly retained, although creation of oxygen vacancy on irradiation reduce the number of unaffected octahedra and leads to progressive disordering of the matrix. At higher fluence ($1 \times 10^{15}/cm^2$) the Raman modes get completely suppressed due to large disorder in the lattice [41]. The XRD and Raman data thus show that the films get progressively disordered on 1 MeV Ar ion irradiation without undergoing any significant structural changes up to a fluence of $5 \times 10^{14}/cm^2$ when the disorder (atomic displacement) is ≈1%.

B. Electronic transport in pristine and disordered films of NNO/STO and NNO/LAO

In this subsection we discuss modifications of resistivities/conductivities arising from progressive disordering of NNO films grown on STO and LAO substrate following the vertical (a) in Fig. 1. In Figs. 5(a) and 5(b) we show the resistivity data for NNO films grown on STO and LAO substrates, respectively. Resistivity data for the pristine NNO films show a change from negative temperature coefficient of resistivity (NTC) to a positive temperature coefficient of resistivity (PTC) as the temperature is lowered. The metal insulator transition temperature (T_{MI}) was identified as a change in the slope of the resistivity. For the NNO/STO film $T_{MI} \approx 180$ K and for the NNO/LAO film $T_{MI} \approx 75$ K. The significant lowering of the T_{MI} in NNO/LAO is due to stabilization of the high temperature metallic phase by compressive strain in the film [30]. The data on the irradiated samples establish *complete suppression* of the MIT by irradiation even at the lowest fluence used (10^{14} cm^{-2}).

As expected in both the pristine $NdNiO_3$ films grown on STO and LAO (i.e., NNO/S0 and NNO/L0), the resistivity in the insulating side below 20 K follows the Mott VRH relation as given in Eq. (1) [42,43]. The data and the fit are given in Figs. S5(a) and S5(b). This is consistent with the earlier results

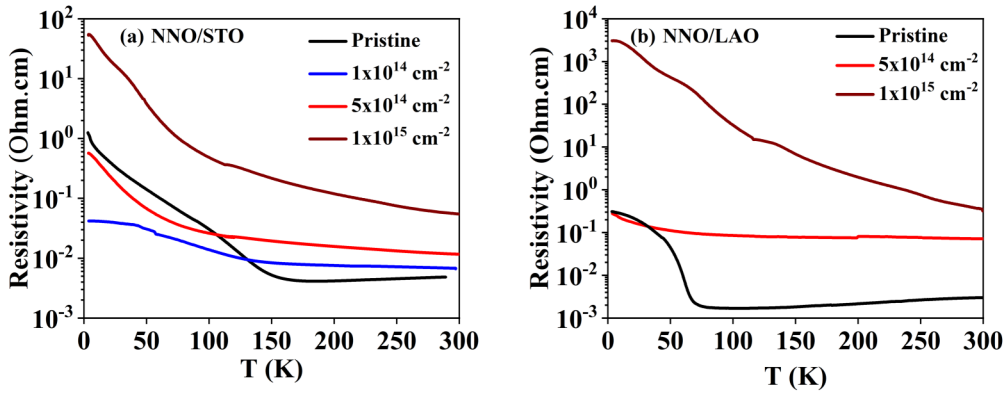

FIG. 5. Resistivity (ρ) as a function of temperature (T) for pristine and irradiated films of NNO grown on (a) STO and (b) LAO substrates.

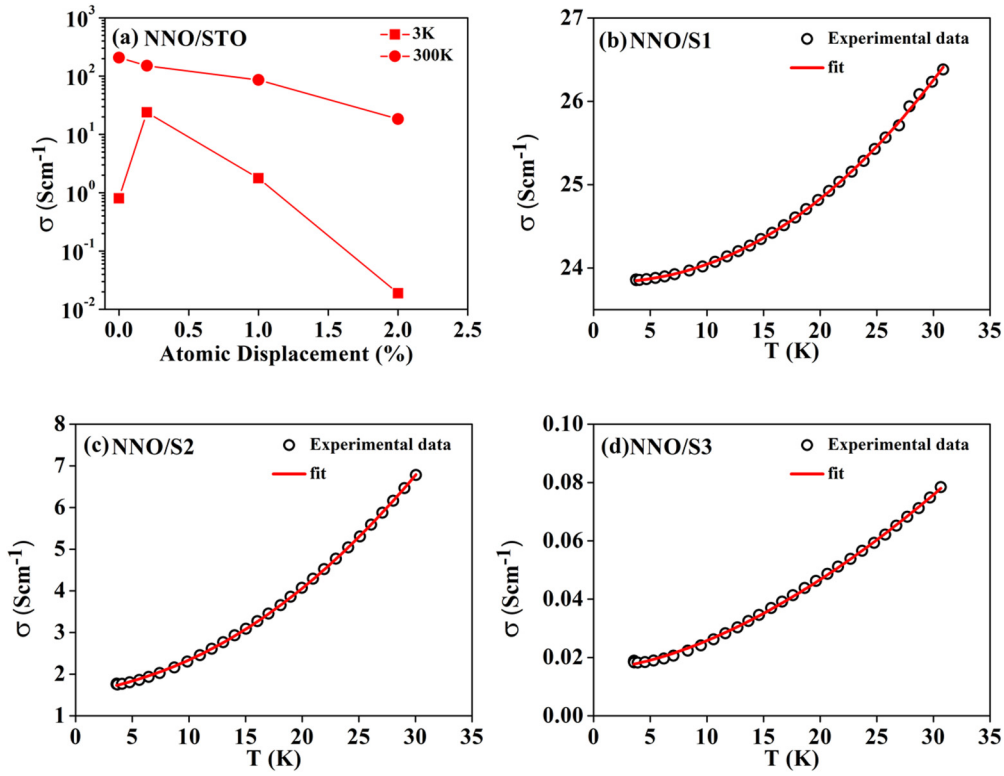

FIG. 6. (a) Evolution of room temperature (300 K) and low temperature (3 K) conductivity (σ) as a function of atomic displacement in NNO/STO film on Ar ion irradiation. (b)–(d) Low temperature power-law dependence of σ on T.

reported for the pristine NNO films [42]:

$$\sigma(T) = \sigma_{0M} T^{-1/4} \exp\left(-\frac{T_0}{T}\right)^{1/4}, \tag{1}$$

where σ_{0M} and T_0 are constants that can be obtained from the fit. T_0 is related to the density of localized states [1,44]. The values extracted from the fits for the NNO/S0 are $\sigma_{0M} = 42.5$ S/cm and $T_0 = 600$ K and the corresponding values for the film NNO/L0 are 18.8 S/cm and 16 K, respectively. We further observe as a test of the insulating nature of the pristine films that for the pristine films, the quantity $W \equiv \frac{d\ln\sigma}{d\ln T}$ diverges as temperature approaches zero [45,46] showing that $\sigma(T = 0) \to 0$ as $T \to 0$. It is noted that $W \to 0$ when the conductivity $\sigma(T = 0)$ reaches a finite value as $T \to 0$. An example of this is shown in Fig. S6 for the NNO/STO films [32].

As stated before, this progressive disordering takes place along the path described by the vertical (a) in Fig. 1. Below we analyze the evolution of the conductivity $\sigma(T)$ of the films on irradiation. In Figs. 6(a) and 7(a) we show the conductivities (σ) at 300 and 3 K for the films grown on STO and LAO as a function of the atomic displacement. (The electrical data are summarized in Table S3 [32].) At 300 K for both films the conductivities progressively decrease on irradiation. This is expected in a conventional solid where disordering by ion irradiation enhances the resistivity. However, startlingly different behaviors are observed at low temperature as shown by the conductivity at $T = 3$ K. In this case there is a nonmonotonous dependence of $\sigma(3\text{ K})$ on disorder. The conductivity of the sample NNO/S1 with 0.2% atomic displacement is higher than that of the pristine sample NNO/S0 by a factor of 30. Even when the fluence is increased by a factor of 5 as in the sample NNO/S2 with atomic displacement of 1%, $\sigma(3\text{ K})$ is higher than that of the pristine sample NNO/S0 by factor of 2.25. For the sample NNO/S3, at higher fluence of radiation leading to larger disorder (atomic displacement of 2%), $\sigma(3\text{ K})$ decreases precipitously and becomes almost 2% of the value of $\sigma(3\text{ K})$ of the pristine sample. The temperature dependence of the conductivities of the irradiated samples are qualitative different from that of the pristine NNO/S0 sample. This establishes that the Mott insulating state with VRH type transport seen in the pristine sample crosses over to a disordered conductor in the irradiated samples that show a power-law conductivity with a finite conductivity at zero temperature. This is shown in Figs. 6(b)–6(d) where we show the conductivities of the irradiated samples NNO/S1, NNO/S2, and NNO/S3 below 30 K where they follow a power law:

$$\sigma(T) = \sigma(0) + AT^m, \tag{2}$$

where $\sigma(0)$ is the conductivity at $T = 0$ K, A and the exponent m are constants. $\sigma(0)$ is considerable for NNO/S1 and it decreases as the fluence increases progressively in NNO/S2 and NNO/S3. The power-law conductivity is expected of a disordered conductor showing WL before it approaches an AI state with a progressively smaller value of $\sigma(0)$. The progressive disordering of the pristine NNO/S0 film thus suppresses the insulating state with a rather low disorder as in the sample NNO/S1 with atomic displacements as low as 0.2% and creates a disordered conductor with WL. Thus the scenario proposed for progressive disordering a Mott insulator to a WL disordered metal following the pathway vertical (a)

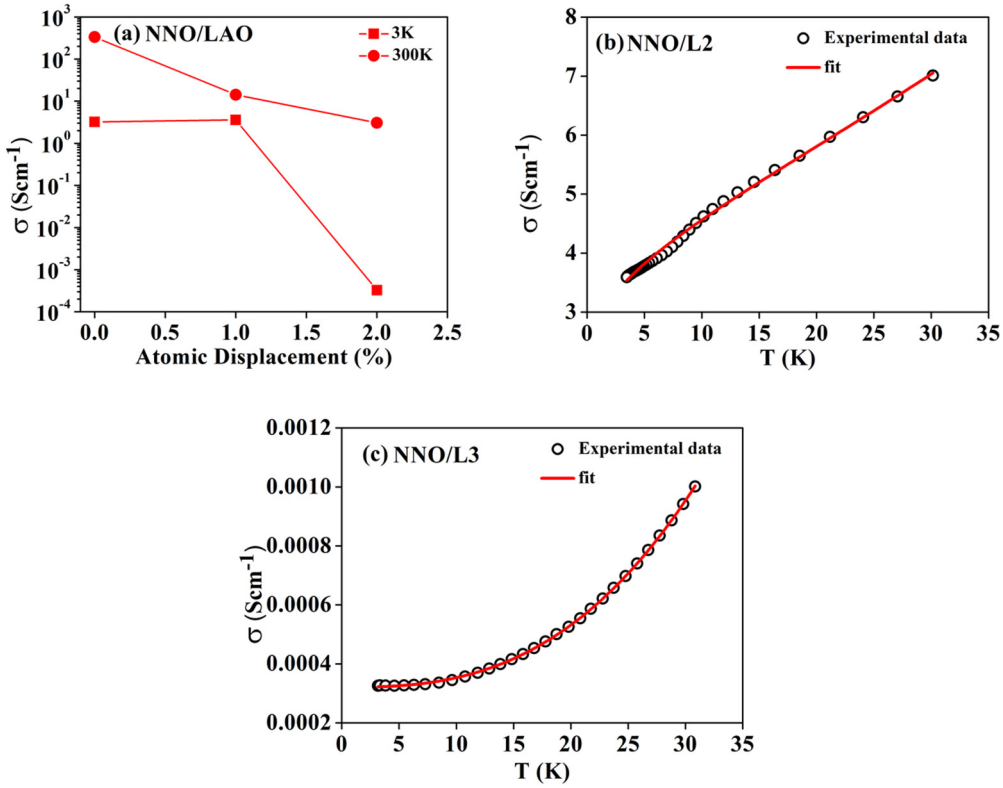

FIG. 7. (a) Evolution of room temperature (300 K) and low temperature (3 K) conductivity (σ) as a function of atomic displacement in NNO/LAO film on Ar ion irradiation. (b) and (c) Low temperature power-law dependence of σ on T.

of Fig. 1 is validated. For the sample NNO/S3 that has highest disorder the $\sigma(0) = 1.6 \times 10^{-2}$ S cm^{-1} is very low to support a metallic state and can be considered to be on the verge of Anderson localization [16,17].

The observation of crossover of a correlation driven insulator by progressive disordering to a disordered metal (likely with WL) and eventually to a highly resistive state but with $\sigma(T = 0) \neq 0$, has also been observed in another set of samples made from the film NNO/LAO. Due to compressive strain in NNO/LAO film the metallic state is stabilized down to lower temperature thus pushing the T_{MI} to much lower temperature and the film has relatively higher conductance than NNO/STO film. The detailed data on the pristine and the irradiated samples are shown in Figs. 7(a)–7(c). The data are summarized in Table S3 [32]. The conductivity of the pristine sample NNO/L0 follows VRH at low temperatures. The progressive disordering by irradiation in the samples NNO/L2 and NNO/L3 follows similar pattern as in the irradiated NNO/STO films where the irradiation induced disordering leads to disordered conductors that show power-law conductivity [Eq. (2)] due to WL and approach disordered induced Anderson localization.

Our observations thus show that the insulating state in $NdNiO_3$ that show a temperature driven MIT like a Mott insulator, on progressive disordering by ion irradiation, does crossover to a disordered conductor with WL and on further disordering moves to a verge of Anderson localization. This has been schematically described in Fig. 1 as the pathway of disordering a Mott insulator along the vertical (a).

C. Radiation induced disordering in NLNO/STO and NLNO/LAO films

In this subsection we compare the radiation induced disordering observed in pristine $NdNiO_3$ films with those observed in a metallic NLNO film grown on LAO or a weakly localized disordered conductor in a film of NLNO grown on STO [28]. Both unirradiated pristine films thus differ qualitatively from the pristine NNO films grown on STO or LAO that show low temperature insulating states. The disordering of the films by 1 MeV Ar irradiation follows path (b) in Fig. 1 and is distinct from the pathway shown by the vertical (a) that has been discussed in the previous section. It has been recently shown by us that in films of NLNO grown on STO and LAO such a substitution can lead to a disordered conducting state with WL which can show a continuous transition to a strongly Anderson localized state [28].

The temperature dependent data for the films of NLNO grown on STO and LAO (pristine and irradiated) are shown in Figs. 8(a) and 8(b), respectively. The data are summarized in Table S3 and can be compared to that data on the NNO/STO and NNO/LAO films (pristine and irrdiated) presented in the previous subsection. The qualitative differences of the pristine NNO films and the NLNO films are noted. However, there are broad similarities in the temperature dependence of the resistivities of the irradiated films. For the NLNO/S0 and NLNO/S1 films the resistivities have shallow negative temperature coefficients (NTC). For the NLNO/S2 and NLNO/S3 films the resistivities have strong NTC and they show behavior of a disordered conductor as elaborated

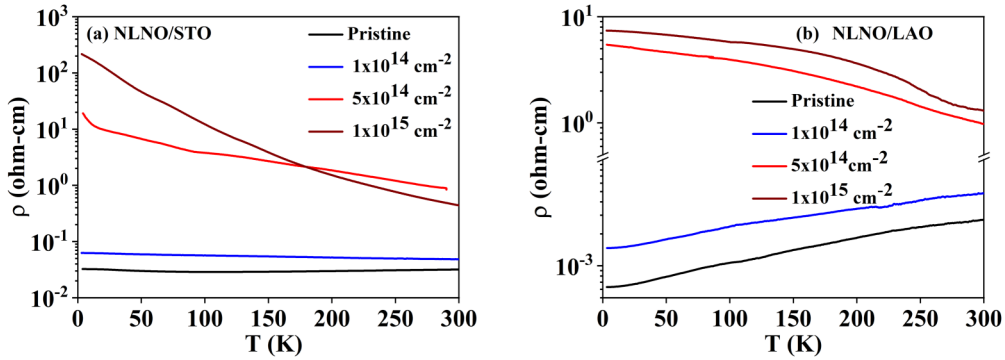

FIG. 8. Resistivity as a function of temperature (T) for pristine and irradiated films of NLNO grown on (a) STO and (b) LAO substrates.

below. For NLNO/LAO films due to compressive stress the pristine sample NLNO/L0 as well as the one irradiated with lowest fluence NLNO/L1 show metallic resistivities with positive temperature coefficients. However, the resistivity in the NLNO/L1 is about 2.5 times higher than that in NLNO/L0. Further disordering causes rapid increase of resistivities and they develop NTC.

Figures 9 and 10, where σ at $T = 3$ and 300 K are shown (see also Table S3), quantify the statements made above for the NLNO/STO and NLNO/LAO films, respectively. For both NLNO/S0 and NLNO/S1 shallow temperature dependence with a small NTC ensures $\sigma(300\ \mathrm{K}) \geqslant \sigma(3\ \mathrm{K})$ while at higher fluences, $\sigma(300\ \mathrm{K}) \gg \sigma(3\ \mathrm{K})$. For all the NLNO/STO films the conductivities follow power law [Eq. (2)] as shown in Fig. S7 and Table S3. The pristine film NLNO/S0 shows considerably high extrapolated zero temperature conductivity $\sigma(0)$, which is higher than NNO/S1, which is obtained after suppressing the Mott insulator. For the NLNO/LO and NLNO/L1, the metallic type temperature dependent resistivities (with positive temperature coefficient) are similar to those observed in a large class of metallic oxides at low temperatures [17] (see Table S3 and Fig. S8). The progressively irradiation turns the metallic behavior to that of a disordered conductor showing power-law conductivity with very low $\sigma(0)$.

We conclude from the above discussion that irradiation creates a disordered conducting state on the verge of Anderson localization whether the starting pristine sample is an insulator like a Mott-insulator following pathway as shown schematically in vertical (a) or a metallic sample with positive temperature coefficient of resistivity following a pathway shown in vertical (b).

D. Noise spectroscopy near MIT and effect of disorder

We have used flicker noise spectroscopy to investigate the effect of irradiation induced disordering on the $NdNiO_3$ film grown on STO. The noise measurement techniques and some of the general issues of noise spectroscopy, relevant for its analysis, have been discussed in Sec. S2 of the Supplemental Material [32]. It has been reported before, including previous investigations done by our group, that a large flicker noise with spectral power density $S(f) \propto \frac{1}{f^{\alpha}}$ appears near the MIT in a correlated electron system like $NdNiO_3$, V_2O_3, and VO_2 [30,31,47–51].

Figures S9(a) and S9(b) show the temperature variations of the two parameters α and the normalized mean square (MS) fluctuation $\frac{\langle \Delta R^2 \rangle}{R^2}$. In the pristine film [see Fig. S9(b)] the exponent $\alpha \approx 1$ away from T_{MI}. However, it shows a sharp

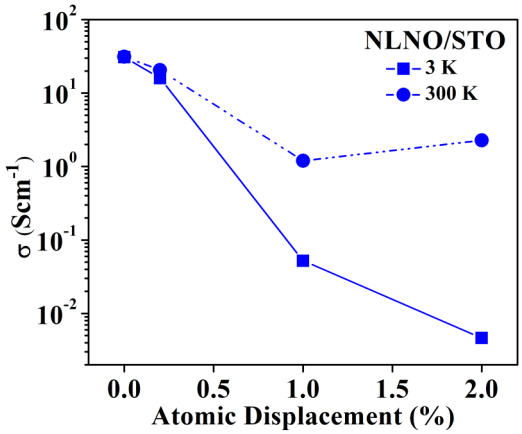

FIG. 9. Dependence on conductivity σ on atomic displacement (%) (fraction of atoms knocked out by heavy ions) at 300 and 3 K for NLNO on STO. Power-law dependence of low temperature conductivity as shown in Fig. S7 of the Supplemental Material [32].

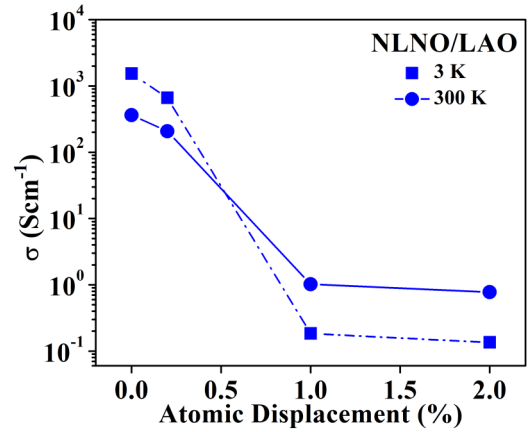

FIG. 10. Dependence on conductivity σ on atomic displacement (%) (fraction of atoms knocked out by heavy ions) at 300 and 3 K for NLNO on LAO. Power -law dependence of low temperature conductivity as shown in Fig. S8 of the Supplemental Material [32].

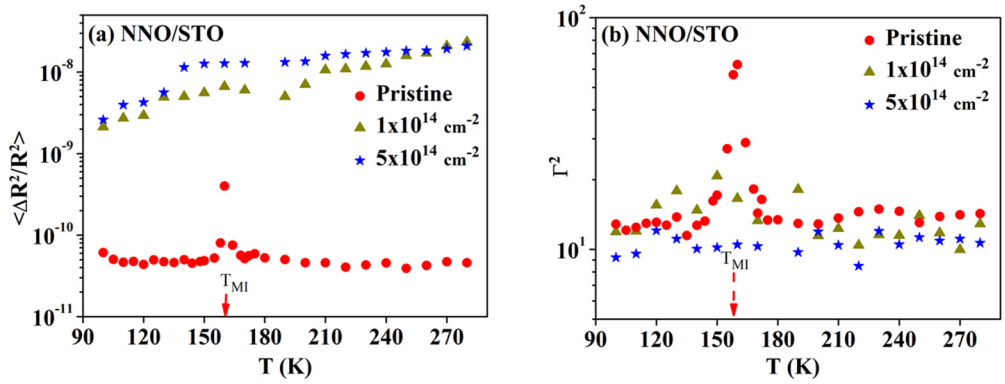

FIG. 11. (a) Normalized mean square resistance fluctuation $\frac{\langle \Delta R^2 \rangle}{R^2}$ and (b) the normalized second spectra Γ^2 of fluctuation as a function of temperature in the pristine and irradiated films of NNO/STO. The metal insulator transition temperature $T_{\rm MI}$ is marked. The data for pristine film has been taken from our past work [31].

rise at $T = T_{\rm MI}$ signifying a shift of the spectral weight to lower frequency. In the irradiated films for $T > T_{\rm MI}$, $\alpha > 1$ signifying dominance of lower frequency fluctuations in the irradiated films. However, at lower temperatures, α show similar temperature dependence as the pristine film, although without a large surge in α at the transition region $T = T_{\rm MI}$.

In Fig. 11(a) the MS fluctuations $\frac{\langle \Delta R^2 \rangle}{R^2}$ are shown for all the films. The pristine films have a nearly temperature independent $\frac{\langle \Delta R^2 \rangle}{R^2}$ except at $T = T_{\rm MI}$, where over a narrow temperature range it shows a surge in the fluctuation by an order of magnitude. In the irradiated films the MS fluctuations are larger than that of the pristine film, which arise from disordering and $\frac{\langle \Delta R^2 \rangle}{R^2}$ has a shallow T dependence as has been observed in metallic oxides films that do not show MIT like $LaNiO_3$ [52,53]. However, due to absence of any discernible signature MIT in them, there is no jump in the MS fluctuations. (See also the Supplemental Material note section S2 [32].)

Absence of a signature of MIT in the irradiated film is also seen in the second spectra shown in Fig. 11(b). In the pristine film Γ^2 for most of the temperature region, it has a shallow temperature dependence and has a value $\approx$12 but at $T \approx T_{\rm MI}$, it jumps to a value as high as 70 due to the appearance of a large non-Gaussian component in the fluctuation. In the irradiated films, Γ^2 have a shallow temperature dependence and have values $\approx$10–12 and there is no signature of a large Γ^2 near MIT unlike the pristine film signifying the absence of significant correlated non-Gaussian fluctuations in the irradiated films.

IV. DISCUSSION

A. Ion irradiation on oxide conductors

The nature of defects created by energetic ions depend on the energy of the ions where lower energy ions create point defects like vacancies and interstitial by nuclear collisions and the higher energy ions with energy well in excess of few MeV generally create extended defects due to electronic excitation and electron energy loss mechanism. In the energy range used by us the predominant energy loss will be by nuclear collisions leading to creation of mainly point defects although there will be some contributions from electronic energy loss.

Formation of defects in oxides formed by energetic ions have been studied extensively for many years [54–57]. The dynamics of defect creation is complex depending on the structure and chemical constituents of the target as well as the energy of the ions used. Nevertheless, there are certain broad features that occur in most oxides. The energetic ions displace atoms into interstitial leaving behind vacancies. In an irradiated solid the top layer of few tens of nanometers, which is of the same order as the thickness of the films used here, the defects created are generally vacancies while deep inside the solid, cascade formation may lead to more complex defect structures which in our case may occur within the substrate [33,58].

In oxides the displacement in the oxygen sublattice is of importance. This leads to creation of three types of vacancies: namely neutral oxygen atom in interstitial, neutral oxygen vacancies, and singly or doubly charged vacancies created by localization of electron within the vacancies. The creation of vacancies thus lead to strong electron localization sites. The randomly placed charged vacancies also act as strong random scatterers which can lead to disordered induced localization as well.

In addition to point defect creation, at higher fluences and ion energy more than few MeV, amorphization can occur beyond a critical temperature of irradiation which is typically >450 K in oxides depending on the ionic radii of the constituent cations [55,56]. In our experiment, the sample is kept mounted on a liquid nitrogen cooled copper plate to avoid heating. As a result it is expected that at extensive amorphization shall not occur in the films. The films predominantly retain their crystalline structure.

A brief gist of past studies on irradiation of $NdNiO_3$ is given below to put our studies in a proper context. Previous studies on thick $NdNiO_3$ films (200 nm) grown on $SrTiO_3$ and $LaAlO_3$ substrates using very high energy (200 MeV) heavy ions (Ag) ions, showed suppression of the $T_{\rm MI}$ and its shift towards smaller temperatures. This has been accompanied by resistivity enhancement [19–21]. In this energy range the fluence used were more than 2 orders less than those used in present work. For ions energy of 200 MeV the defect created are not point defects and have extended nature. In these studies mainly the enhancement of resistivities on ion irradiation were investigated. However, the issue of suppression of the

MIT and the insulating state and its crossover to a disordered conductor with WL and eventual approach to Anderson localized state have not been addressed. The observations were explained as arising from strains created by irradiation.

B. Nature of electrical conduction in the irradiated films at low temperature

The evolution of the low temperature conductivity σ ($T \leqslant 30$ K) in the disordered conducting state that evolves on progressive disordering by ion irradiation follows a power law following Eq. (2). The evolution of the exponent m on disordering and on approach to Anderson localized state would need comments. Power-law conductivity of ABO_3 perovskite disordered oxides close to Anderson MI transition driven by substitutional doping has been investigated by our group in the past. In substitutional systems like $LaNi_{1-x}Co_xO_3$, Na_xWO_3, $La_{1-x}Sr_xO_3$, exponent $0.5 \leqslant m \leqslant 1$. However, in the La doped $NdNiO_3$ system, namely $Nd_{0.7}La_{0.3}NiO_3$, the exponent $1 \leqslant m \leqslant 2$. The evolution in the exponent m can arise in such disordered systems from relative weights of the WL term (that adds a correction to conductivity) as well as from an electron-electron interaction term (EEI). While the EEI term contributes a $\sqrt{T}$ temperature to conductivity, the contribution from the WL contribution comes from the term correction to conductivity that depends on the temperature dependent phase coherence length $L_\phi(T)$ given as [3]

$$\delta\sigma_{\mathrm{WL}}(T) = \frac{e^2}{2\pi^2\hbar}\left(\frac{1}{L_\phi(T)}\right). \tag{3}$$

The temperature dependence of $L_\phi(T)$ depends on the scattering mechanism which arises from the relation $L_\phi(T) = (D\tau_\phi)^{1/2}$ where D is the electron diffusivity and τ_ϕ is the phase relaxation time. Generally $\tau_\phi \propto T^p$ with $1.5 < p < 4$. When the phase relaxation is dominated by electron-electron scattering $1.5 < p < 2$ and when it is dominated by electron-phonon scattering $2 < p < 4$. The observed m will thus be $\approx \frac{p}{2}$. In our experiment $1 < m < 2$ showing that the predominance of the scattering arises from the electron-phonon scattering which is expected in the temperature range of the study as well as strong electron-phonon coupling in the oxide systems. Taking into account both the EEI contribution and the WL contribution we write the temperature dependence of σ at $T \leqslant 30$ K as [17]

$$\sigma_{(T)} = \sigma_0 + A\sqrt{T} + BT^2. \tag{4}$$

In Figs. S10(a) and S10(b) we show some representative examples to fit Eq. (4). The variation of the exponent m can thus be considered to arise from relative changes in weight of the the two contributions that changes as the disorder changes the electron diffusivity D. The progressive disordering reduces $\sigma(0)$ significantly and changes m as well. The low values of $\sigma(0)$ for the samples with highest disorder signifies that they are most likely approaching a disordered induced localized insulating state with $\sigma(0) \to 0$.

The samples that have undergone irradiation with highest fluences though have low conductivity (high resistivity) do not show a clear insulating behavior (activated transport) unlike the pristine samples which show a VRH type of conduction [Eq. (1)]. Instead, these samples show a conductivity that show power-law behavior [Eq. (2)] with a finite conductivity $\sigma(0)$ as $\to 0$. While this is expected in samples that show weak localization or approach Anderson insulator state, a small value of $\sigma(0)$ in the range of 10^{-2} to 5×10^{-3} S/cm would need comments. This value of $\sigma(0)$ is much less than those of Mott minimum conductivities (σ_{Mott}) observed in disordered oxides [17] that are typically in the range of $\sigma_{\mathrm{Mott}} \leqslant 100$ S/cm. It is noted that a low value of $\sigma(0) \leqslant 10$ S/cm has also been observed in $Nd_{0.7}La_{0.3}NiO_3$ system as it passes through a region of substitution induced continuous MI transition [28]. A low value of $\sigma(0)$ may arise from two sources. It may arise from very low DOS at E_F which may happen since the collapse of the insulating state would involve filling of the gap in the DOS at the Fermi level. It may happen that the onset of strong disorder makes the samples inhomogeneous leading to coexisting insulating and conducting (albeit with low conductivity) regions. It has been shown in the context of rare-earth manganites that the presence of a minority phase conducting region at low temperatures in the majority phase of a insulating solid can lead to a situation at low T where the current is predominantly carried in the regions of higher conductivities which can lead to a finite $\sigma(0)$ [59].

V. SUMMARY

To summarize, we show that the ion irradiation induced disorder in an insulator like $NdNiO_3$, which is like a Mott insulator, can lead to collapse of the insulating state and a crossover to a disordered conductor which due to progressing disordering approaches Anderson localization. It has been argued that radiation induced disordering may be a cleaner way to disorder a correlated insulator as the more conventional process of disordering by ionic substitution may bring in additional factors.

It is a conventional wisdom that when a solid is disordered it leads to lowering (raising) of conductance (resistance). We however, make a counterintuitive observation that at lower fluence at low T the conductivity enhances on irradiation. This arises, as discussed before, on the collapse of the insulating state on disordering. It has also been observed, using noise spectroscopy, that in the irradiated films the non-Gaussian content of the resistance fluctuation that arises due to the correlated nature of the fluctuation in pristine films, and shows up clearly at $T \approx T_{\mathrm{MI}}$, is suppressed.

ACKNOWLEDGMENTS

The work has been supported by a sponsored project from the Science and Engineering Research Board (SERB), Government of India (ref: EMR/2016/002855/ PHY). A.K.R. wants to thank SERB for Distinguished Fellowship (ref: SB/DF/008/2019). R.S.B. thanks Anusmita Chakravorty and Kedar Mal for their help during the ion irradiation.

[1] N. F. Mott, *Metal-Insulator Transition* (Taylor and Francis, London, 1990).

[2] M. Imada, A. Fujimori, and Y. Tokura, Rev. Mod. Phys. **70**, 1039 (1998).

[3] P. A. Lee and T. V. Ramakrishnan, Rev. Mod. Phys. **57**, 287 (1985).

[4] P. P. Edwards, R. L. Johnston, C. N. R. Rao, D. P. Tunstall, and F. Hensel, Phil. Trans. R. Soc. London Sect. A **356**, 5 (1998).

[5] P. Edwards and C. N. R Rao, Eds., *Metal-Insulator Transitions Revisited* (Taylor and Francis, Bristol, 1995).

[6] R. E. Peierls, *Quantum Theory of Solids* (Oxford University Press, New, York, 1955), p. 108.

[7] N. F. Mott, Proc. Phys. Soc. A **62**, 416 (1949).

[8] N. F. Mott, Rev. Mod. Phys. **40**, 677 (1968).

[9] P. W. Anderson, Phys. Rev. **109**, 1492 (1958).

[10] F. Evers and A. D. Mirlin, Rev. Mod. Phys. **80**, 1355 (2008).

[11] D. Belitz and T. R. Kirkpatrick, Rev. Mod. Phys. **66**, 261 (1994).

[12] K. Byczuk, W. Hofstetter, and D. Vollhardt, Phys. Rev. Lett. **94**, 056404 (2005).

[13] H. Bragança, M. C. O. Aguiar, J. Vučičević, D. Tanasković, and V. Dobrosavljević, Phys. Rev. B **92**, 125143 (2015).

[14] A. E. Antipov, Y. Javanmard, P. Ribeiro, and S. Kirchner, Phys. Rev. Lett. **117**, 146601 (2016).

[15] D. I. Khomskii, *Transition Metal Compounds* (Cambridge University Press, Cambridge, 2014).

[16] C. N. R. Rao and J. Gopalakrishnan, *New Directions in Solid State Chemistry* (Cambridge University Press, 1997), p. 200.

[17] A. K. Raychaudhuri, Adv. Phys. **44**, 21 (1995).

[18] T. Sasaki, Crystals **2**, 374 (2012).

[19] Y. Kumar, R. J. Choudhary, A. P. Singh, G. Anjum, and R. Kumar, J. Appl. Phys. **108**, 083706 (2010).

[20] Y. Kumar, R. J. Choudhary, and R. Kumar, J. Appl. Phys. **112**, 073718 (2012).

[21] Y. Kumar, R. J. Choudhary, and R. Kumar, J. Appl. Phys. **120**, 115306 (2016).

[22] S. Middey, J. Chakhalian, P. Mahadevan, J. W. Freeland, A. J. Millis, and D. D. Sarma, Annu. Rev. Mater. Res. **46**, 305 (2016).

[23] S. Catalano, M. Gibert, J. Fowlie, J. Iguez, J. M. Triscone, and J. Kreise, Rep. Prog. Phys. **81**, 046501 (2018).

[24] H. Park, A. J. Millis, and C. A. Marianetti, Phys. Rev. Lett. **109**, 156402 (2012).

[25] I. I. Mazin, D. I. Khomskii, R. Lengsdorf, J. A. Alonso, W. G. Marshall, R. M. Ibberson, A. Podlesnyak, M. J. Martinez-Lope, and M. M. Abd-Elmeguid, Phys. Rev. Lett. **98**, 176406 (2007).

[26] V. Bisogni, S. Catalano, R. J. Green, M. Gibert, R. Scherwitzl, Y. Huang, V. N. Strocov, P. Zubko, S. Balandeh, J.-M. Triscone, G. Sawatzky, and T. Schmitt, Nat. Commun. **7**, 13017 (2016).

[27] A. S. Disa, D. P. Kumah, J. H. Ngai, E. D. Specht, D. A. Arena, F. J. Walker, and C. H. Ahn, APL Mater. **1**, 032110 (2013).

[28] R. S. Bisht, G. N. Daptary, A. Bid, and A. K. Raychaudhuri, J. Phys.: Condens. Matter **31**, 145603 (2019).

[29] Z. Wang, Y. Okada, J. O'Neal, W. Zhou, D. Walkup, C. Dhital, T. Hogan, P. Clancy, Y.-J. Kim, Y. F. Hu, L. H. Santosa, S. D. Wilson, N. Trivedi, and V. Madhavana, Proc. Natl. Acad. Sci. **115**, 11198 (2018).

[30] R. S. Bisht, S. Samanta, and A. K. Raychaudhuri, Phys. Rev. B **95**, 115147 (2017).

[31] S. Chatterjee, R. S. Bisht, V. R. Reddy, and A. K. Raychaudhuri, Phys. Rev. B **104**, 155101 (2021).

[32] See Supplemental Material at http://link.aps.org/supplemental/10.1103/PhysRevB.105.205120 for the full range XRD and low temperature fitting for different films.

[33] J. F. Ziegler, J. P. Biersack, and M. D. Ziegler, *SRIM—The Stopping and Range of Ions in Matter* (Ion Implantation Press, 2008).

[34] J. H. Scofield, Rev. Sci. Instrum. **58**, 985 (1987).

[35] A. K. Raychaudhuri, Curr. Opin. Solid State Mater. Sci. **6**, 67 (2002).

[36] A. Ghosh, S. Kar, A. Bid, and A. K. Raychaudhuri, arXiv:cond-mat/0402130.

[37] F. X. Zhang, H. Xue, J. K. Keum, A. Boulle, Y. Zhang, and W. J. Weber, J. Phys. Condens. Matter **32**, 355405 (2020).

[38] M. Zaghrioui, A. Bulou, P. Lacorre, and P. Laffez, Phys. Rev. B **64**, 081102(R) (2001).

[39] C. Girardot, J. Kreisel, S. Pignard, N. Caillault, and F. Weiss, Phys. Rev. B **78**, 104101 (2008).

[40] J. Fowlie, B. Mundet, C. Toulouse, A. Schober, M. Guennou, C. Domínguez, M. Gibert, D. T. L. Alexander, J. Kreisel, and J.-M. Triscone, APL Mater. **9**, 081119 (2021).

[41] M. Zhang, Raman study of the crystalline-to-amorphous state in alpha-decay–damaged materials, http://dx.doi.org/10.5772/65910.

[42] A. Stupakov, O. Pacherova, T. Kocourek, M. Jelinek, A. Dejneka, and M. Tyunina, Phys. Rev. B **99**, 085111 (2019)

[43] K. Ramadoss, N. Mandal, X. Dai, Z. Wan, Y. Zhou, L. Rokhinson, Y. P. Chen, J. Hu, and S. Ramanathan, Phys. Rev. B **94**, 235124 (2016).

[44] R. M. Hill, Phys. Status Solidi (a) **34**, 601 (1976).

[45] A. Möbius, Crit. Rev. Solid State Mater. Sci. **44**, 1 (2019).

[46] W. N. Shafarman, D. W. Koon, and T. G. Castner, Phys. Rev. B **40**, 1216 (1989).

[47] S. Samanta, A. K. Raychaudhuri, X. Zhong, and A. Gupta, Phys. Rev. B **92**, 195125 (2015).

[48] A. Sahoo, S. D. Ha, S. Ramanathan, and A. Ghosh, Phys. Rev. B **90**, 085116 (2014).

[49] A. M. Alsaqqa, S. Singh, S. Middey, M. Kareev, J. Chakhalian, and G. Sambandamurthy, Phys. Rev. B **95**, 125132 (2017).

[50] G. N. Daptary, S. Kumar, M. Kareev, J. Chakhalian, A. Bid, and S. Middey, Phys. Rev. B **100**, 125105 (2019).

[51] S. Kundu, T. Bar, R. K. Nayak, and B. Bansal, Phys. Rev. Lett. **124**, 095703 (2020).

[52] A. Ghosh, A. K. Raychaudhuri, R. Sreekala, M. Rajeswari, and T. Venkatesan, J. Phys. D (Appl. Phys.) **30**, L75 (1997).

[53] A. Ghosh and A. K. Raychaudhuri, Phys. Rev. B **64**, 104304 (2001).

[54] E. A. Kotomin and A. I. Popov, Nucl. Instrum. Methods Phys. Res. B **141**, 1 (1998).

[55] K. E. Sickafus, L. Minervini, R. W. Grimes, J. A. Valdez, M. Ishimaru, F. Li, K. J. McClellan, and T. Hartmann, Science **289**, 748 (2000).

[56] K. E. Sickafus, R. W. Grimes, J. A. Valdez, A. Cleave, M. Tang, M. Ishimaru, S. M. Corish, C. R. Stanek, and B. P. Uberuaga, Nat. Mater. **6**, 217 (2007).

[57] M. M. Rahaman, W.-Y. Chen, L. Mu, Z. Xu, Z. Xiao, M. Li, X.-M. Bai, and F. Lin, Nat. Commun. **11**, 4548 (2020).

[58] J. F. Ziegler, J. Biersack, and U. Littmark, *The Stopping and Range of Ions in Matter* (Pergamon, New York, 1985).

[59] T. Sarkar, A. K. Raychaudhuri, A. K. Bera, and S. M. Yusuf, New J. Phys. **12**, 123026 (2010).